



CHAPTER V
BENZIMIDAZOLE MODEL COMPOUNDS AND THEIR CONSEQUENT
MOLECULAR PACKING STRUCTURES FOR HYDROGEN BOND
NETWORK CHANNELS

5.1 Abstract

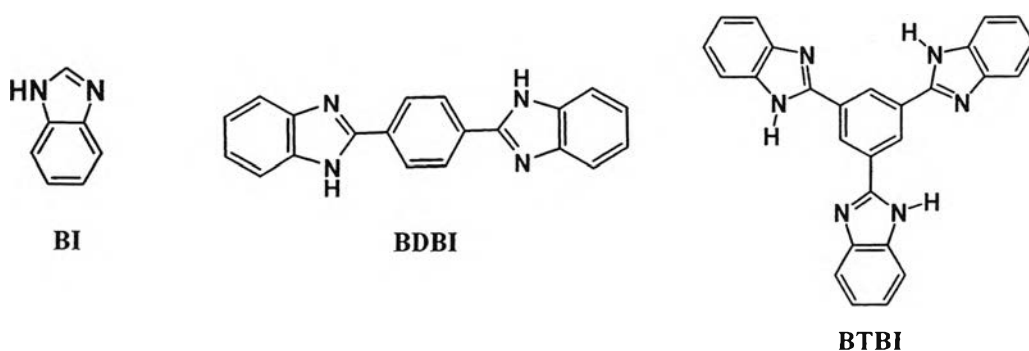
A systematical study on benzimidazole-based molecules, i.e., mono-, di- and tri-functional benzimidazole, and their molecular packing structures are carried out. The increase in benzimidazole unit is found to strongly affect the structure of hydrogen bond network from the “isolated channel type” to the “layered interlinked channel type”. When the solvent molecules involved in the packing structure, the hydrogen bond between benzimidazole and solvent molecules gives “solvent assisted network”; however, this obstructs the intermolecular hydrogen bonding among benzimidazoles. The present work is a guideline to understand hydrogen bond network and its proton transfer possibility so as to develop an as-desired benzimidazole functional polymer.

Keywords: Benzimidazole, Heterocycles, Proton Conductivity, Proton Transfer, PEMFC, Fuel Cell.

5.2 Introduction

During the past few years, the development of proton-conducting membrane for polymer electrolyte membrane fuel cell (PEMFC) has focused on the application of the membrane at intermediate temperature (100-200°C) where many advantages could be expected, i.e., improving carbon monoxide tolerance of the Pt electrode, accelerating the electrochemical reaction on the catalyst, enhancing proton mobility through the electrolyte membrane, giving higher energy efficiency with heat managements and cogenerations, etc.¹ However, the commercially available electrolyte membranes, such as humidified Nafion, are unsatisfied under this condition due to the evaporation of water molecules, which play a role as the proton carriers, out of the membranes at temperature higher than 100°C.² Thus, an alternative proton conduction system based on the heteroaromatic compounds, such as imidazole, benzimidazole and pyrazole, were introduced.³ Unfortunately, most of the researches concern only about the application of those functional group in polymeric membrane with whereas the points about how the proton transfer is favored and what molecular design should be are still left behind. Most studies mentioned about the orientation of the heterocyclic resonance and its consequent hydrogen bond networks.⁴ Taking this into our consideration, we believe that building up a well-defined structure and understand the proton transfer route based on the specific molecular arrangement is a good approach to develop the material and achieve the goal.

Scheme 5.1 Structures of BI, BDBI, and BTBI.



On this viewpoint, the present work is a part of our continuing work on benzimidazole-based proton transfer functional polymer. Here, we focus on an understanding of molecular packing structure and its hydrogen bond network based on a systematical study on benzimidazole model compounds with mono-, di- and tri-functional benzimidazole, i.e., benzimidazole (BI), 1,4-benzenedi-2-benzimidazole (BDBI), and 1,3,5-benzenetri-2-benzimidazole (BTBI), respectively (Scheme 6.1).

5.3 Experimental

5.3.1 Materials

1,3,5-benzenetri-2-benzimidazole, BTBI, was synthesized as reported in our previous work (Chapter III). Benzimidazole (BI) was purchased from Aldrich, Germany. Terephthaoyl chloride and 1,2-phenylenediamine were obtained from Wako, Japan. All chemicals were analytical grade and used without further purification.

5.3.2 Instruments and Equipments

FT-IR spectra were recorded on a Thermo Nicolet Nexus 670 Fourier transform infrared spectrophotometer at a resolution of 2 cm^{-1} in a frequency range of $4000\text{-}400\text{ cm}^{-1}$, using a deuterated triglycinesulfate detector (DTGS). Temperature dependent FTIR spectroscopy was performed with an in-house temperature-controlled sample holder. Proton nuclear magnetic resonance ($^1\text{H NMR}$) spectra were collected by a Varian Mercury-400BB spectrometer using tetramethylsilane as an internal standard and DMSO-d_6 as a solvent. Thermogravimetric analyses (TGA) were performed by a Perkin Elmer TGA7 thermogravimetric analyzer under nitrogen atmosphere with a flow rate of 20 ml/min and scanning temperature at $50\text{-}900^\circ\text{C}$ with a scanning rate of 10°C/min .

5.3.3 Preparation of BDBI

The steps of reactions are summarized in Scheme 5.2. Terephthaloylchloride (0.2310 g , $8.53\times 10^{-4}\text{ mol}$) in xylene (150 ml) was added

dropwisely into a vigorously stirred solution of 1,2-phenylenediamine (0.3820 g, 3.51×10^{-3} mol) in xylene (50 ml) at 70°C under nitrogen atmosphere. The red brownish precipitates were obtained after overnight. The precipitates were collected and dissolved in 1-methyl-2-pyrrolidone (NMP). The solution was refluxed at 150°C under vacuum for 24 h to obtain yellow precipitates. The product was washed several times with distilled water and methanol before kept drying in vacuum to obtain *1,2-Benzenedi-2-benzimidazole*, BDBI.

Characterization: FT-IR (cm⁻¹): 3200-2500 (strong, hydrogen bonded N-H stretching); 1440 (strong, skeleton vibration of benzimidazole ring); 743 (strong, aromatic C-H bending). ¹H NMR (DMSO-d₆): δ_H 8.35 (4H, s, Ar-H (benzene)); 7.40 (4H, d, Ar-H (benzimidazole)); 7.20 (4H, d, Ar-H (benzimidazole)). Elemental analysis (%) Found: C 77.74. H 4.26. N 17.90. Calcd. for C₂₀H₁₄N₄: C 77.42. H 4.52. N 18.06. MALDI-TOF MS (CCA, positive, m/z): 310.64; FW of C₂₀H₁₄N₄: 310; T_m (°C): 474; T_d (°C): 530; Yield (%): 58.6. Single crystals necessary for X-ray structure analysis were prepared by recrystallization in DMSO and sublimation at 300 °C under reduced pressure.

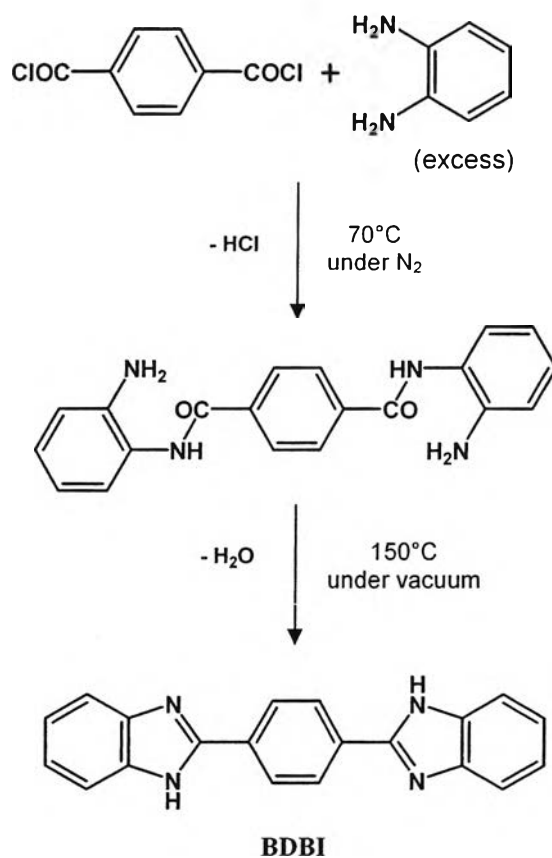
5.4 Results and Discussion

5.4.1 Preparation of Benzimidazole-based Model Compounds

Synthesis of BTBI was reported in our previous work (Chapter III), whereas BI is a commercial product provided by Aldrich. For BDBI, the similar synthesis procedure to that of BTBI was applied. The use of NMP instead of ethylene glycol in the second step allows us to skip the step of neutralizing an intermediate compound obtained from the first step reaction. This is because NMP is a base solvent which can abstract proton from the intermediate compound and recover the nucleophilicity of the remaining amino groups. The success of preparing BDBI could be confirmed by the similar FTIR spectrum as those of BI and BTBI (Figure 5.1). The absorption bands at 3200-2500 cm⁻¹ refer to the characteristic peaks of N-H···N stretching of diazole ring. The strong peaks at 1440 and 743 cm⁻¹ belong to skeleton vibration of benzimidazole ring and C-H bending of aromatic ring, respectively. ¹H NMR spectrum of BDBI also shows the peaks at 8.35, 7.40 and 7.20

ppm which relate to the 4 protons on benzene core and 8 protons on benzimidazole ring, respective (Figure 5.2). Mass spectrum (Figure 5.3) reveals the parent peak (M+1) at 310.64 m/z representing the molecular weight of BDBI (FW of $C_{20}H_{14}N_4$ is 310). Elemental analysis also supports the structure of BDBI with the related result between the observed data (C 77.74, H 4.26, N 17.90) and the calculated one (Calcd. for $C_{20}H_{14}N_4$: C 77.42, H 4.52, N 18.09).

Scheme 5.2 Synthesis of 1,4-benzenedi-2-benzimidazole, BDBI.



5.4.2 Solvent-involved Molecular Packing Structures Observed in Benzimidazole-based Model Compounds

Molecular arrangement of the compounds studied by X-ray structural analysis of single crystal can give us the direct information about atomic position in the crystal lattice which further indicate the molecular packing structure and hydrogen bonds in the compound. Here, solution-recrystallization technique was

applied to grow single crystals of BDBI and BTBI, while structure of BI crystal prepared by this technique was already reported by Vijayan *et. al.* as an orthorhombic crystal system under $Pna2_1$ with four molecules in the unit cell (Figure 5.4).^[5]

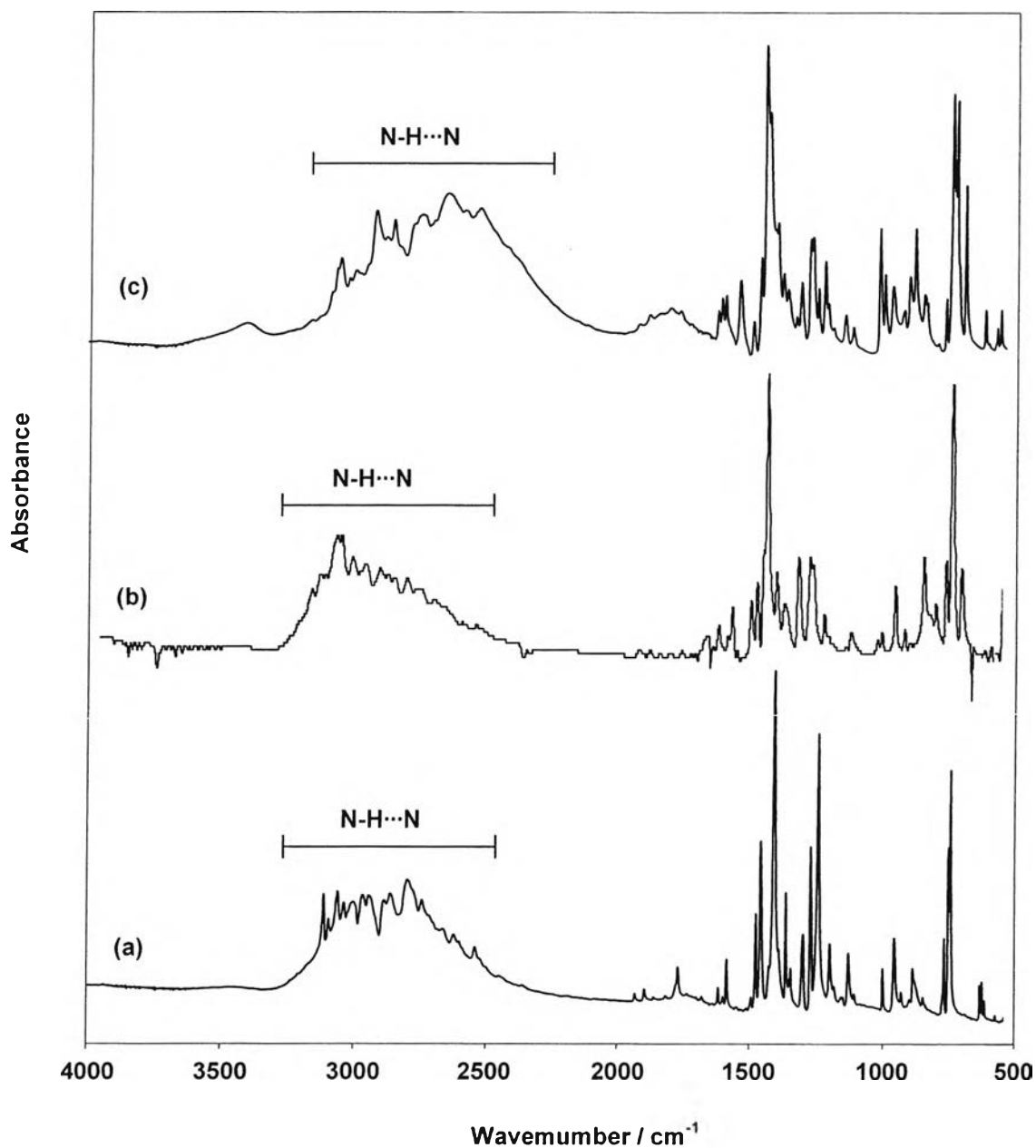


Figure 5.1 FTIR spectra of BI (a), BDBI (b), and BTBI (c).

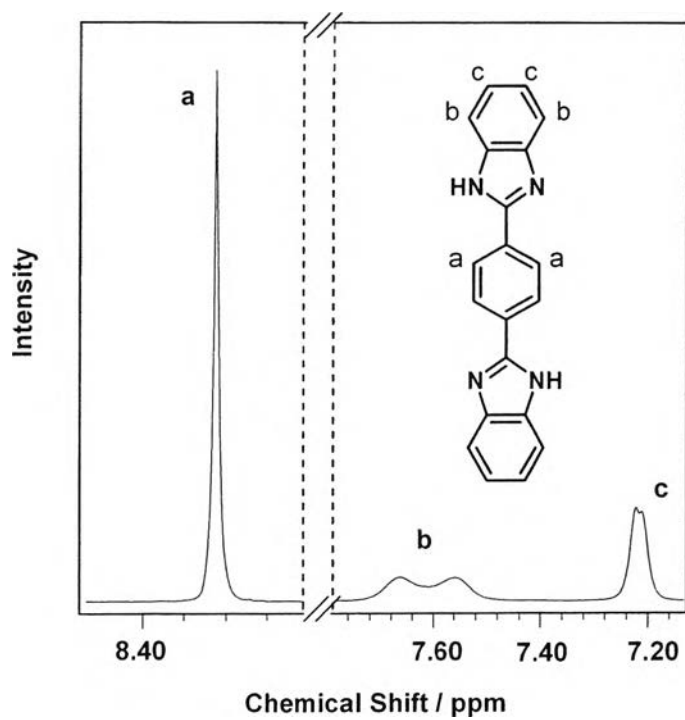


Figure 5.2 ^1H NMR spectrum of BDBI.

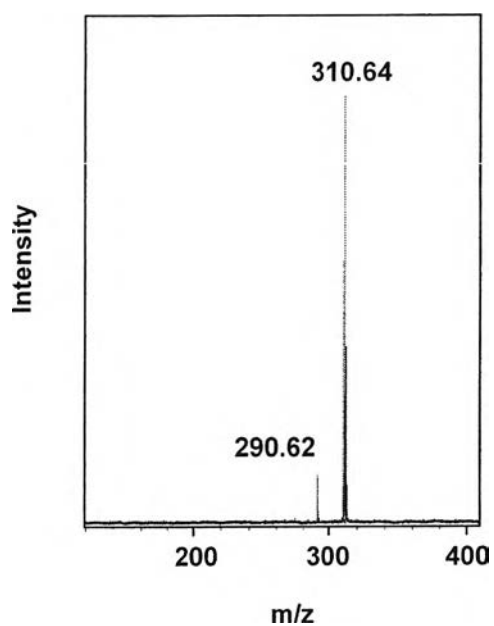


Figure 5.3 MALDI-TOF mass spectrum of BDBI.

There, they showed that BI molecules are aligned with a specific NH...N distance between the adjacent molecules $\sim 2.8 \text{ \AA}$ which is relevant to hydrogen bond interaction. The hydrogen bonds link the neighboring molecules together to generate the channel of hydrogen bond network along the BI molecules which can be considered as an ideal system for proton conduction. This work is a good for us when we focus on the molecular packing structure induced hydrogen bond network derived by benzimidazole compound.

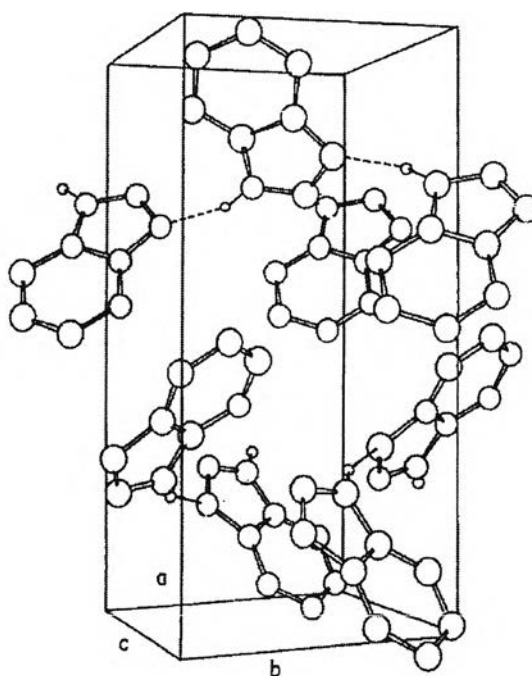


Figure 5.4 Crystal structure of benzimidazole proposed by Vijayan *et. al.*⁵

Single crystals of BDBI and BTBI were prepared by recrystallization in good solvents, i.e., DMSO and 2-propanol for BDBI and BTBI, respectively. Figure 5.5 shows the crystal structures of BDBI and BTBI crystals. In both cases, the incorporation of solvent molecules in the crystal lattice can be observed. For BDBI (Figure 5.5 (a)), the composition of BDBI and DMSO is in the ratio of 1:2. The molecular conformation of BDBI appears to be the planar shape structure. Moreover, an appropriate NH...O distance between BDBI and the nearest solvent molecule is found to be around 2.8 \AA reflecting hydrogen bond interactions.

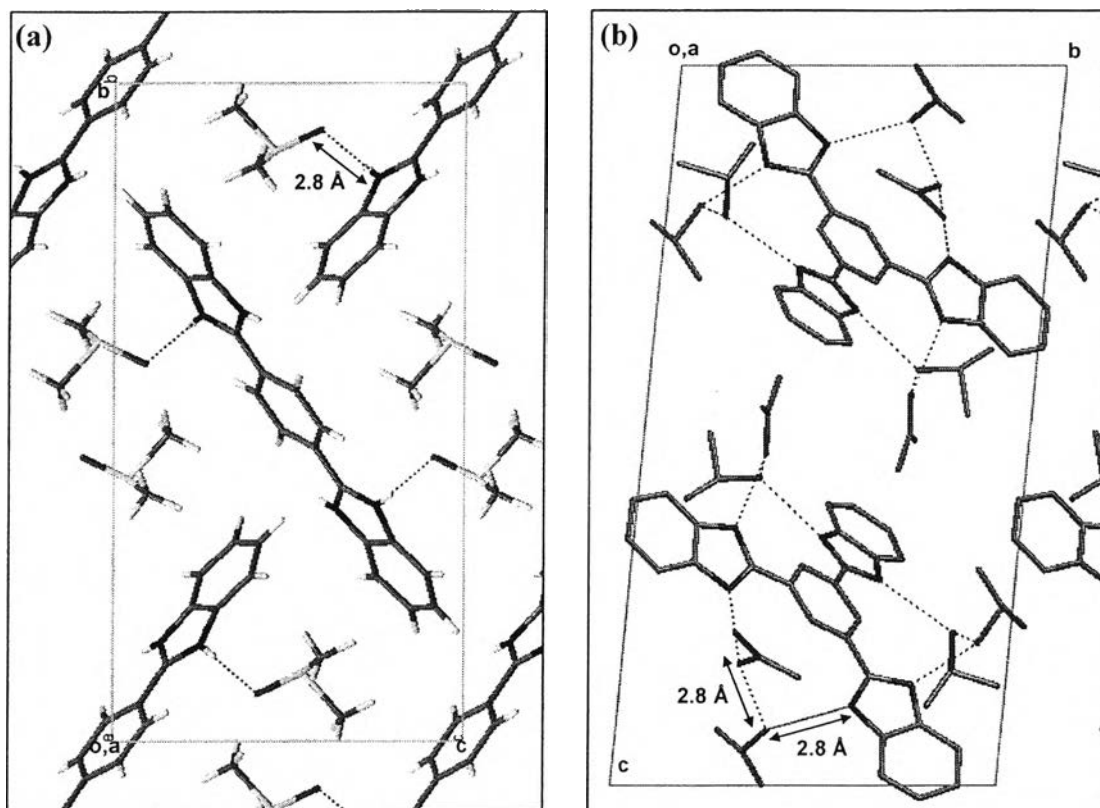


Figure 5.5 Crystal structures obtained from solution-recrystallized crystals: BDBI in DMSO (a), and BTBI in 2-propanol (b).^{7,8}

However, it is important to note that the planar packing with solvent molecules obstruct the formation of intermolecular hydrogen bond among the BDBI molecules. This might not be an ideal case when we consider the proton transfer along the hydrogen bond network of benzimidazole units. In the case of BTBI, although 2-propanol in the crystal might disturb the intermolecular hydrogen bond, it generates another unique hydrogen bond network between all three benzimidazole units (Figure 5.5 (b)). Here, we term it as a “solvent-assisted intramolecular hydrogen bond network”.⁵ But this type of hydrogen bond network, again, might not be effective for proton transfer in PEMFC.

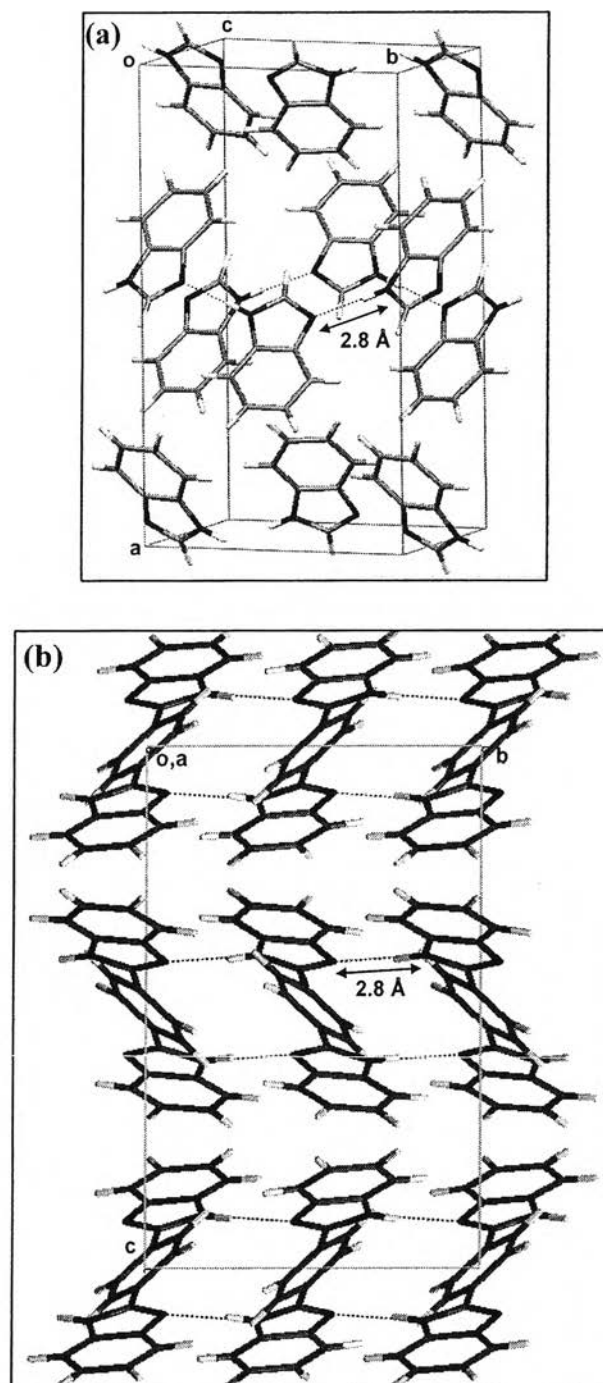


Figure 5.6 Crystal structures of BI (a), and BDBI (b).^{7,8}

5.4.3 Hydrogen Bond Network Channels Generated by Molecular Packing Structures of Pristine Benzimidazole Compounds

An effort to prepare single crystals without solvent molecules was accomplished by sublimation. Figure 5.6 illustrates the crystal structures of BI and

BDBI observed from the sublimed crystals. For both crystals, the specific distance related to hydrogen bond ($\sim 2.8 \text{ \AA}$) of $\text{NH}\cdots\text{N}$ between the adjacent molecules could be extracted. In other words, both molecules are aligned with a regular hydrogen bond network. Considering the point of hydrogen bond network channel, we could figure out the significant differences between these two hydrogen bond network systems as shown in Figure 5.7. For crystal structure of BI, the molecules are aligned side-by-side with hydrogen bond interaction to generate the channel of hydrogen bond network. Here, we term it as “isolated channel of hydrogen bond network” as shown in Figure 5.7 (a).⁵

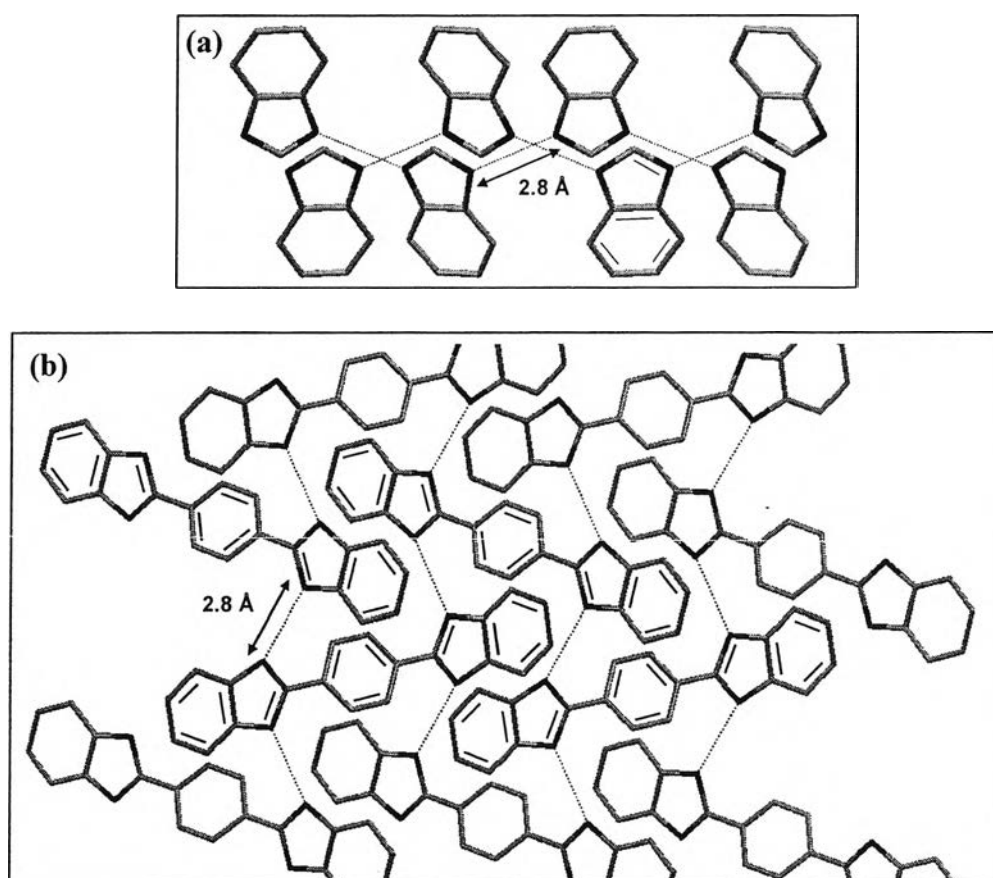


Figure 5.7 Channels of hydrogen bond networks in crystal structures (hiding hydrogen atom): isolated channel of hydrogen bond network observed in BI crystal (a), and layered interlinked channels of hydrogen bond networks observed in sublimed BDBI crystal (b).⁷ For better understanding, double bonds are added up over the CIF images.

On the other hand, the molecular packing structure of pristine BDBI gives the hydrogen bond networks under the same layer which are connected together to generate a “layered-interlinked channel of hydrogen bond network” as illustrated in Figure 5.7 (b).

Therefore, it is clear that the number of benzimidazole unit on molecule can controls the structure of hydrogen bond network. Furthermore, as the molecular conformation of BDBI is changed from planar shape to non-planar one after removing solvent molecules, this suggests that solvent molecules are not only affect the packing structure and hydrogen bond network formation but also the molecular conformation of the compounds. In the case of BTBI, the sublimation was carried out several times; however, the single crystal appropriate for single crystal analysis was yet to be achieved

In this way, the results indicate that benzimidazole compounds show high possibility to induce the formation of hydrogen bond network functioning as proton transferring route. The modification of benzimidazole-based compounds might lead to the unique hydrogen bond network that offers us a significant improvement in proton transfer property.

5.5 Conclusion

A series of mono-, di- and tri-functional benzimidazole derivatives was developed as model compounds. The studies on their crystal structures via X-ray structural analyses demonstrated the formation of hydrogen bond network channels derived by the molecular packing and hydrogen bond interaction of the model compounds. The work revealed that by increasing the number of benzimidazole unit from mono- to di-functional benzimidazole, the structure of hydrogen bond network was changed from the “isolated channel type” to the “layered interlinked channel type”. Solvent molecules were also found to significantly affect the hydrogen bond network as they initiated a unique “solvent-assisted intramolecular hydrogen bond network” in BTBI but obstruct the formation of intermolecular hydrogen bond network in BDBI.

5.6 Acknowledgement

The authors would like to acknowledge The National Research Council of Thailand (NRTC), Japan Society for the Promotion of Science (JSPS), The Engineering Research and Development Project (National Metal and Materials Technology Center, Thailand), and Research Task Force Program (Chulalongkorn university). P. E. would like to thank The Development and Promotion of Science and Technology Talent Project (DPST) for her scholarship. P. T. and S. C. wish to extend their gratitude to The Thailand Research Fund (TRF) for the RGJ-Ph.D. scholarship (grant no. PHD/0031/2547).

5.7 References and Notes

- (1). M. Yamada, I. Honma, *J. Phys. Chem. B* **2004**, *108*, 5522.
- (2). D. J. Jones, J. Rozière, *J. Membr. Sci.* **2001**, *185*, 41.
- (3). K. D. Kreuer, A. Fuchs, M. Ise, M Spaeth, J. Maier, *Electrochim. Acta* **1998**, *43 (10-11)*, 1281.
- (4). M. Münch, K. D. Kreuer, W. Silvestri, J. Maier, G. Seifert, *Solid State Ionics* **2001**, *145*, 437.
- (5). N. Vijayan, N. Balamurugan, R. Ramesh Babua, R. Gopalakrishnana, P. Ramasamy, W.T.A. Harrison, *Journal of Crystal Growth*, **2004**, *267*, 218.
- (6). Characterizations. **BDBI** FTIR (KBr, cm^{-1}): 3200-2500 (N-H (diazole ring)), 1440 (skeleton vibration (benzimidazole)), 743 (C-H (aromatic)); ^1H NMR (400 MHz, d_6 -DMSO, ppm): δ_{H} 8.35 (4H, s, Ar-H), 7.40 (4H, d, Ar-H), 7.20 (4H, d, Ar-H); EA (%) Found: C 77.74, H 4.26, N 17.90; Calcd for $\text{C}_{20}\text{H}_{14}\text{N}_4$: C 77.42, H 4.52, N 18.06; MALDI-TOF MS (CCA, positive, m/z): 310.64; FW of $\text{C}_{20}\text{H}_{14}\text{N}_4$: 310; Tm ($^{\circ}\text{C}$): 474; Yield (%): 58.6. **BTBI** FTIR (KBr, cm^{-1}): 3000-2400 (N-H (diazole ring)), 1444 (skeleton vibration (benzimidazole)), 743 (C-H (aromatic)); ^1H NMR (400 MHz, CD_3OD , ppm): δ_{H} 8.76 (3H, s, Ar-H); 7.62 (6H, broad, Ar-H); 7.24 -7.27 (6H, dd, Ar-H); EA (%) Found: C 73.37, H 4.91, N 18.55. Calcd.

For $C_{27}H_{18}N_6$: C 76.06, H 4.23, N 19.72.; ESI-MS (positive, m/z): 427.16; FW of $C_{27}H_{18}N_6$: 310; Tm ($^{\circ}C$): 445; Yield (%): 68.8.

- (7). Crystal structure images were acquired from CIF files using Mercury (Hg) Program.
- (8). Crystal Structures. **BI** (CCDC 675661): orthorhombic (Pccn); a=16.6754 Å, b=9.7372 Å, c=7.6219 Å; V=1237.6 Å³; Z=8; R1=0.0445. **BDBI with DMSO**: monoclinic (P2₁/n); a=5.827 Å, b=19.370 Å, c=10.323 Å; V=1165.3 Å³; Z=4; R1=0.0486. **Pristine BDBI**: orthorhombic (Pbca); a=10.266 Å, b=9.748 Å, c=14.960 Å; V=1497.2 Å³; Z=4; R1=0.0714. **BTBI with 2-propanol** (CCDC 671942): triclinic (P-1); a=9.081 Å, b=11.991 Å, c=22.376 Å; $\alpha=95.13^{\circ}$, $\beta=93.04^{\circ}$, $\gamma=95.52^{\circ}$; V=2394.2 Å³; Z=2; R1 (without adding hydrogen)=0.1098.